

Electrostatically Tuned Interactions in Silica Microsphere–Polystyrene Nanoparticle Mixtures

Angel T. Chan and Jennifer A. Lewis*

Frederick Seitz Materials Research Laboratory, Materials Science and Engineering
Department, University of Illinois, Urbana, Illinois 61801

Received April 14, 2005. In Final Form: July 26, 2005

We explore the generality of nanoparticle haloing¹ as a novel colloidal stabilization mechanism in binary mixtures of silica microspheres and polystyrene nanoparticles. By selectively tuning their electrostatic interactions, both the initial microsphere stability and the role of nanoparticle additions are varied. Adsorption isotherm and zeta potential measurements indicate that highly charged nanoparticles exhibit a weak (haloing) association with negligibly charged microspheres, whereas they either strongly adsorb onto oppositely charged or are repelled by like-charged microsphere surfaces, respectively. Bulk sedimentation and confocal scanning fluorescence microscopy reveal that important differences in system stability emerge depending on whether the added nanoparticles serve as haloing, bridging, or depletant species.

We previously identified a new colloidal stabilization mechanism,^{1,2} known as “nanoparticle haloing”, in silica microsphere–hydrated zirconia nanoparticle mixtures that possess both high charge and size asymmetry. On the basis of experimental observations, we proposed that these highly charged nanoparticles preferentially segregate to regions near the negligibly charged microsphere surfaces because of their repulsive Coulombic interactions in solution, thus mitigating the van der Waals attraction that drives microsphere aggregation in their absence.^{1,2} Recent theoretical³ and simulation^{4,5} efforts support the idea that dynamic halos arise in such systems, leading first to their stabilization above a critical nanoparticle concentration and, ultimately, to their gelation at even higher nanoparticle concentrations by a mechanism that may differ qualitatively from regular depletion attraction. However, the underlying mechanism(s) that foster nanoparticle haloing remains a subject of debate. For example, Liu and Luijten^{4,5} report that a weak electrostatic attraction (approx. several kT in magnitude) between microsphere–nanoparticle species is necessary to induce such phenomena. When this was explicitly accounted for in their simulations, they made predictions that were in good agreement with our experimental findings.^{1,2,6} In contrast, Karanikas and Louis³ found that nanoparticle haloing can be driven solely by an electrostatic repulsion between nanoparticles in solution; however, a significantly larger Debye screening length (i.e., higher effective nanoparticle concentration) was required to match our original experimental results. Because these prior observations were confined to a single experimental system whose complex solution chemistry is less than ideal for interpreting the rich behavior observed, there is a critical need to investigate the behavior of other binary mixture with similar charge and size asymmetry.

Here, we explore the generality of nanoparticle haloing in a model system composed of silica microspheres and

polystyrene nanoparticles whose mutual electrostatic interactions can be tuned by varying the solution pH and nanoparticle surface functionalization. These binary mixtures contain silica microspheres (Geltech, Alachua, FL) and either sulfate or amidine polystyrene (PS) nanoparticles (IDC, Portland, OR). Specifically, three binary mixtures are studied: (1) strongly attractive, (2) weak, and (3) strongly repulsive, as classified by their microsphere–nanoparticle interactions (Table 1).

The microsphere–microsphere, nanoparticle–nanoparticle, and microsphere–nanoparticle interaction potentials for these binary mixtures are shown in Figure 1. These potentials are calculated using Derjaguin–Landau–Verwey–Overbeek (DLVO) theory, in which the van der Waals (vdW) potential^{7–9} is determined by Lifshitz theory¹⁰ and the electrostatic interactions are calculated using the linear superposition approximation (LSA)^{7,11–13} (Supporting Information). When the microspheres are negligibly charged, vdW interactions dominate leading to their net attraction. In contrast, when the microspheres are highly charged, there is a strong electrostatic repulsion between such species. The highly charged nanoparticles, present in each mixture, exhibit a strong electrostatic repulsion with an effective size of $\sim 2.5a_{\text{nano}}$ (i.e., an effective nanoparticle volume fraction, $\phi_{\text{eff}} = 0.156\phi_{\text{nano}}$). Finally, the microsphere–nanoparticle interactions are highly attractive or repulsive in mixtures possessing opposite- or like-charged species, respectively, whereas a weak repulsion ($\sim 1 kT$) that precedes a modest attractive well (approx. several kT in magnitude) is predicted for mixtures composed of negligibly charged microspheres and highly charged nanoparticles. Such differences strongly influence the adsorption, sedimentation, and phase behavior observed for each binary mixture.

To quantify the extent of nanoparticle adsorption on the microsphere surfaces, we prepared binary mixtures

* Corresponding author. E-mail: jalewis@uiuc.edu.

(1) Tohver, V.; Chan, A.; Sakurada, O.; Lewis, J. A. *Langmuir* **2001**, *17*, 8414–8421.

(2) Tohver, V.; Smay, J. E.; Braem, A.; Braun, P. V.; Lewis, J. A. *Proc. Natl. Acad. Sci. U.S.A.* **2001**, *98*, 8950–8954.

(3) Karanikas, S.; Louis, A. A. *Phys. Rev. Lett.* **2004**, *93*, 248303.

(4) Liu, J.; Luijten, E. *Phys. Rev. Lett.* **2004**, *93*, 247802.

(5) Liu, J.; Luijten, E. *Phys. Rev. Lett.* **2004**, *92*, 035504.

(6) Martinez, C. J.; Liu, J.; Rhodes, S. K.; Luijten, E.; Weeks, E. R.; Lewis, J. A. *Langmuir*, published online April 19, <http://dx.doi.org/10.1021/la050382s>.

(7) Hunter, R. J. *Foundations of Colloid Science*; Oxford University Press: New York, 1987; Vol. I.

(8) Israelachvili, J. *Intermolecular and Surface Forces*, 2nd ed.; Academic Press: San Diego, CA, 1991.

(9) Lewis, J. A. *J. Am. Ceram. Soc.* **2000**, *83*, 2341–2359.

(10) Prieve, D. C.; Russel, W. B. *J. Colloid Interface Sci.* **1988**, *125*, 1–13.

(11) Bell, G. M.; Levine, S.; McCartney, L. N. *J. Colloid Interface Sci.* **1970**, *33*, 335–359.

(12) Warszynski, P.; Adamczyk, Z. *J. Colloid Interface Sci.* **1997**, *187*, 283–295.

(13) Ohshima, H.; Healy, T. W.; White, L. R. *J. Colloid Interface Sci.* **1982**, *90*, 17–26.

Table 1. Material Properties of Microsphere–Nanoparticle Mixtures^a

strongly attractive	weakly interacting	strongly repulsive
$2a_{\text{micro}} = 1.18 \pm 0.02 \mu\text{m}$	$2a_{\text{micro}} = 1.18 \pm 0.02 \mu\text{m}$	$2a_{\text{micro}} = 1.18 \pm 0.02 \mu\text{m}$
$\zeta_{\text{micro}} = -40 \text{ mV}$	$\zeta_{\text{micro}} = -1 \text{ mV}$	$\zeta_{\text{micro}} = -40 \text{ mV}$
$2a_{\text{nano}} = 21 \pm 5 \text{ nm}$	$2a_{\text{nano}} = 19 \pm 3 \text{ nm}$	$2a_{\text{nano}} = 19 \pm 3 \text{ nm}$
$\zeta_{\text{nano}} = 95 \text{ mV}$	$\zeta_{\text{nano}} = -120 \text{ mV}$	$\zeta_{\text{nano}} = -120 \text{ mV}$
pH 5, 1mM NaNO ₃	pH 3	pH 5, 1 mM NaNO ₃

^a Note: 1 mM sodium nitrate salt (NaNO₃) was added to maintain a constant Debye screening length (κ^{-1}) of 9.6 nm.

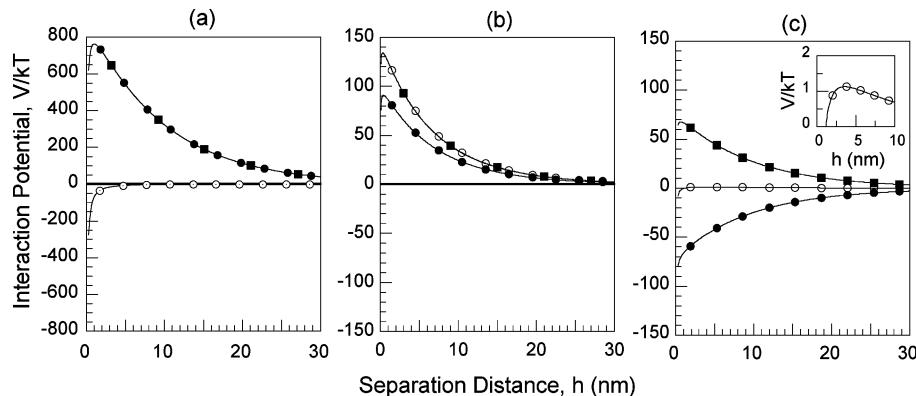


Figure 1. Total interparticle interaction potential as a function of separation distance between (a) microsphere–microsphere, (b) nanoparticle–nanoparticle, and (c) microsphere–nanoparticle species in the strongly attractive (●), weakly interacting (○) and strongly repulsive (■) binary mixtures. The inset in (c) depicts a magnified view of the weakly interacting system.

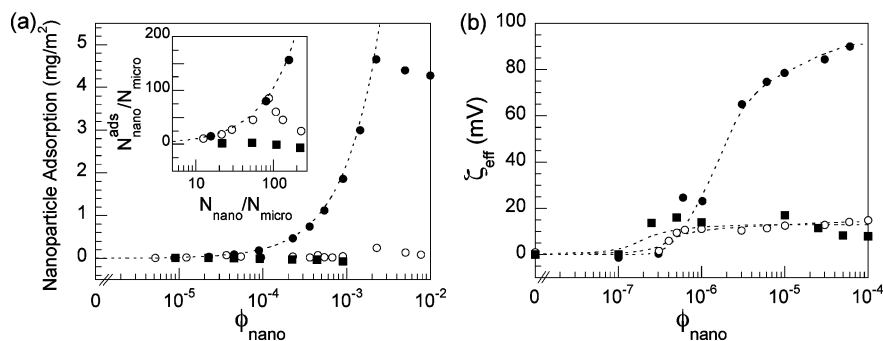


Figure 2. (a) Fluorometric analysis of nanoparticle adsorption onto silica microsphere surfaces in binary mixtures ($\phi_{\text{micro}} = 10^{-1}$) as a function of nanoparticle volume fraction and (b) the effective microsphere zeta potential as a function of nanoparticle volume fraction for the strongly attractive (●), weakly interacting (○), and strongly repulsive (■) mixtures ($\phi_{\text{micro}} = 10^{-5}$). The inset in (a) depicts a magnified view of the nanoparticle adsorption behavior plotted as a function of the number ratio of adsorbed nanoparticles per microsphere ($N_{\text{nano}}^{\text{ads}}/N_{\text{micro}}$) vs those in solution ($N_{\text{nano}}/N_{\text{micro}}$). The dotted line in (a) depicts 100% adsorption.]

($\phi_{\text{micro}} = 1 \times 10^{-1}$ and $\phi_{\text{nano}} = (0-1) \times 10^{-2}$) of each system with fluorescently labeled PS nanoparticles and analyzed the fluorescence intensity of the corresponding supernatant solutions after the microspheres settled from each suspension under gravity. As shown in Figure 2a, when the microsphere–nanoparticle species interact weakly, the extent of nanoparticle adsorption is negligible. The inset (Figure 2a) reveals that the nanoparticles quickly reach a rather modest plateau value of 0.05 mg/m² (~50 nanoparticles per microsphere). This corresponds to a nanoparticle packing fraction of only 0.004 with a minimum (lateral) separation distance of 320 nm—nearly an order of magnitude greater than the effective nanoparticle size. In sharp contrast, there is a significant adsorption of nanoparticles on the microsphere surfaces when their mutual attraction is strengthened (Figure 2a). A plateau coverage of 4.5 mg/m² is observed for the strongly attractive mixtures, which corresponds to ~3750 nanoparticles per microsphere and a packing fraction of ~0.39. This yields a minimum (lateral) separation distance between nanoparticles of 20 nm. At this close proximity, the nanoparticle species exhibit a modest (lateral) electrostatic repulsion. However, their ability to pack to such high density is likely facilitated by their strong attraction to the underlying

microsphere surface. As expected, when the net repulsion between microsphere–nanoparticle species is greatly enhanced, no nanoparticle adsorption is observed.

To further probe the extent of nanoparticle association with the microsphere surfaces, we measured the effective microsphere zeta potential (ζ_{eff}) as a function of nanoparticle volume fraction for each binary mixture ($\phi_{\text{micro}} = 1 \times 10^{-5}$ and $\phi_{\text{nano}} = 0-1 \times 10^{-4}$). To enable direct comparison of the data shown in Figure 2b, ζ_{eff} is plotted in terms of the absolute magnitude of the difference between the measured microsphere zeta potential in the presence and absence of nanoparticle species. Thus, ζ_{eff} contains contributions from both bare and nanoparticle-coated regions on the microsphere surfaces. The measured zeta potential is related to the surface charge (Q) of a particle by the Loeb equation¹⁴

$$Q = 4\pi\epsilon_0 \frac{kT}{ze} \kappa a^2 \left\{ 2 \sinh\left(\frac{ze\zeta}{2kT}\right) + \frac{4}{\kappa a} \tanh\left(\frac{ze\zeta}{4kT}\right) \right\} \quad (1)$$

where kT is the thermal energy, z is the charge of the ions

(14) Hunter, R. J. *Zeta Potential in Colloid Science: Principles and Applications*; Academic Press Inc.: New York, 1981.

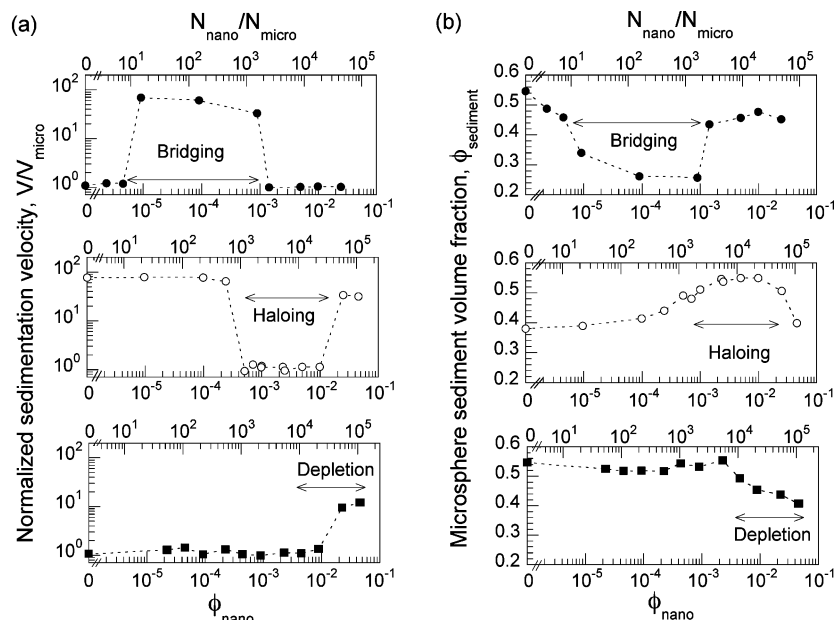


Figure 3. (a) Normalized initial sedimentation velocity (V/V_{micro}) from bulk sedimentation and (b) microsphere sediment volume fraction as a function of nanoparticle volume fraction for the strongly attractive (\bullet), weakly interacting (\circ), and strongly repulsive (\blacksquare) binary mixtures ($\phi_{\text{micro}} = 10^{-1}$), where V_{micro} is the sediment velocity calculated for an individual microsphere in water.

in solution, e is the electron charge, $\epsilon\epsilon_0$ is the dielectric constant of the solution, κ^{-1} is the Debye screening length (9.6 nm), and a is the particle radius. From these data, the number of nanoparticles associated with each microsphere is calculated. When microsphere–nanoparticle species interact either weakly or with a strong repulsion, the effective microsphere zeta potential exhibits a modest rise of 14 mV, from which we estimate that ~ 175 nanoparticles per microsphere is needed to induce the observed charge buildup. The effective microsphere zeta potential exhibits a substantial rise of 90 mV (from -40 to 50 mV) with increasing nanoparticle volume fraction when the microsphere–nanoparticle interactions are strongly attractive. From these data, we estimate that ~ 2000 nanoparticles per microsphere are needed to induce this giant charge reversal. This value is in reasonable agreement with the maximum nanoparticle coverage determined from adsorption measurements (Figure 2a).

The above data for mixtures of negligibly charged silica microspheres and highly charged PS nanoparticles are strikingly different from our prior observations on silica–hydrous zirconia mixtures,^{1,2,6} in which the extent of nanoparticle association was not only more appreciable ($\sim 10\%$ of those free in solution) but also increased with increasing nanoparticle concentration, leading to a more pronounced rise in the effective microsphere zeta potential. We attribute such differences to two important factors. First, there are subtle variations in the microsphere–nanoparticle interactions between the two experimental systems. Most notably, a modest repulsive barrier ($\sim 1 kT$) is predicted to precede an attractive well (several kT in magnitude) for the silica–PS mixtures, whereas only an attractive well (of approximately the same value) is calculated for the silica–hydrous zirconia mixtures.³ Second, the PS nanoparticles are more highly charged, which when coupled with the 5-fold increase in the Debye length in solution yields a larger effective nanoparticle size and, thus, a larger effective volume fraction. Hence, repulsive interactions between nanoparticles in solution may play a more prominent role in halo formation in the present system. An obvious question therefore is whether PS nanoparticle additions will induce microsphere stabilization above a critical nanoparticle volume fraction

analogous to our earlier findings despite these underlying differences in their adsorption behavior.

To probe suspension stability, we investigated the effects of nanoparticle additions on the initial microsphere sediment volume fraction, and morphology of each binary mixture ($\phi_{\text{micro}} = 1 \times 10^{-1}$ and $\phi_{\text{nano}} = 0\text{--}5 \times 10^{-2}$), as shown in Figures 3 and 4. In the absence of nanoparticles, negligibly charged microspheres flocculate and settle rapidly, producing an open sediment ($\phi_{\text{sediment}} = 0.37$), whereas the highly charged microspheres are stable and settle individually to form a dense polycrystalline sediment ($\phi_{\text{sediment}} = 0.55$). Upon adding nanoparticles, the system behavior varies dramatically.

When microsphere–nanoparticle species interact weakly, there is a sharp decrease in microsphere sediment velocity and a concurrent rise in sediment density at a lower critical nanoparticle volume fraction ($\phi_{\text{L,C}}$) of $\sim 6 \times 10^{-4}$. Above $\phi_{\text{L,C}}$, the microspheres settle individually, assembling into a face-centered cubic array that is polycrystalline in nature (Figure 4b), a hallmark of a fully stabilized system. If the microsphere–nanoparticle interactions are greatly intensified in either direction (attractive or repulsive), then the resulting binary mixtures exhibit more classical behavior due to nanoparticle-induced bridging^{15–17} or depletion^{18–20} flocculation. For example, bridging flocculation occurs in the strongly attractive mixtures, giving rise to a 100-fold increase in the microsphere sediment velocity and very open sediment structures (Figures 3 and 4). Ultimately, as the nanoparticle volume fraction increases, each microsphere becomes well coated with highly charged nanoparticles, leading to microsphere restabilization by electrosteric effects. In contrast, strongly repulsive binary mixtures

(15) Dumont, F.; Ameryckx, G.; Watillon, A. *Colloids Surf.* **1990**, *51*, 171–188.

(16) Harley, S.; Thompson, D. W.; Vincent, B. *Colloids Surf.* **1992**, *62*, 153–162.

(17) Islam, A. M.; Chowdhry, B. Z.; Snowden, M. J. *Adv. Colloid Interface Sci.* **1995**, *62*, 109–136.

(18) Jenkins, P.; Snowden, M. *Adv. Colloid Interface Sci.* **1996**, *68*, 57–96.

(19) Walz, J. Y.; Sharma, A. *J. Colloid Interface Sci.* **1994**, *168*, 485–496.

(20) Sharma, A.; Tan, S. N.; Walz, J. Y. *J. Colloid Interface Sci.* **1997**, *190*, 392–407.

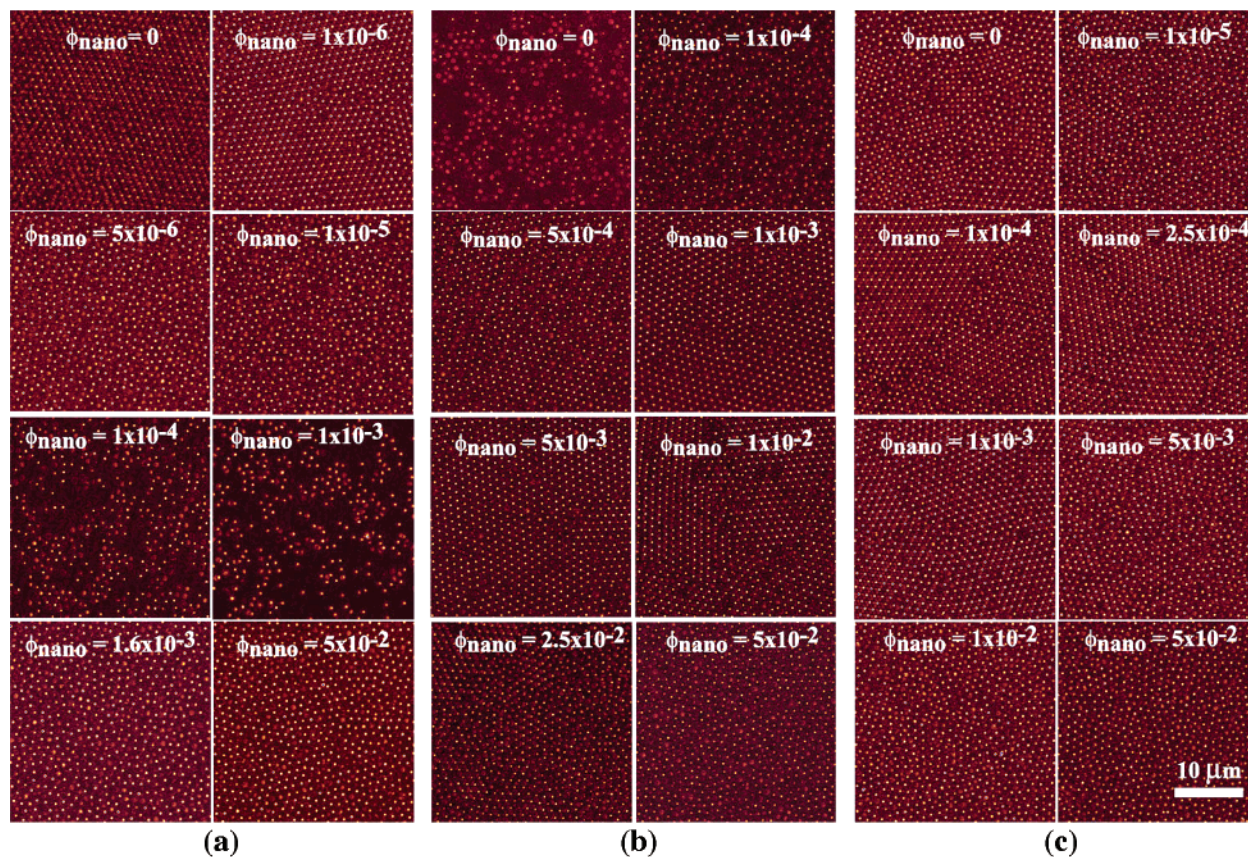


Figure 4. Confocal images (x - y scans) of colloidal microspheres assembled from binary mixtures of varying nanoparticle volume fraction under gravity-driven sedimentation: (a) strongly attractive, (b) weakly interacting, and (c) strongly repulsive mixtures.

remain stable over a broad range of ϕ_{nano} before eventually destabilizing when ϕ_{nano} exceeds $\sim 10^{-2}$. We attribute the observed flocculation to entropic depletion interactions that arise between the microspheres due to the highly charged nanoparticles.^{18–20}

The phase behavior of binary mixtures composed of negligibly charged silica microspheres and highly charged PS nanoparticles is nearly identical to observations reported for the original haloing system,⁶ thus some commonality in the underlying stabilization mechanism is inferred. Because the degree of nanoparticle association is far less in the present system, we believe that repulsive nanoparticle interactions in solution do indeed play a more pronounced role. For example, the “window of stability” determined from the sedimentation experiments ranges from $\phi_{\text{nano}} \approx 6 \times 10^{-4}$ to 10^{-2} (corresponding to $\phi_{\text{eff}} \approx 0.01$ – 0.16). This translates to a nanoparticle-to-microsphere number ratio in solution for microsphere stabilization that far exceeds the maximum adsorption of ~ 50 nanoparticles per microsphere measured for this system (Figure 2). Of course, it is possible that this value does not accurately reflect the extent of halo formation when the microspheres are fully suspended in these weakly interacting mixtures. Interestingly, the onset of re-entrant gelation observed for these mixtures nearly coincides with the nanoparticle concentration required to induce depletion flocculation in strongly repulsive mixtures. Clearly, our current observations further highlight the rich complexity that arises in binary mixtures of negligibly charged microspheres and highly charged nanoparticles. Additional experimental, simulation, and theoretical efforts are needed to fully elucidate the effects of individual particle size and charge, size and charge ratio, and solution composition on the magnitude and range over which one can tune the

interactions between species while still residing within a dynamic haloing regime for a given system.

In summary, the effects of electrostatically tuned interactions on the phase behavior and assembly of binary mixtures composed of silica microspheres and polystyrene nanoparticles have been investigated. We have demonstrated the generality of nanoparticle haloing as a novel colloidal stabilization mechanism in a model experimental system. We have also identified important differences in the phase behavior between the three types of binary mixtures studied and have shown that it depends on both the initial microsphere stability and whether the added nanoparticles serve as bridging, haloing, or depleting species. An open question that emerges from this work is over what magnitude and range one can tune the interactions between such species and still reside in a weak (dynamic haloing) regime. Further studies are now underway to explore the phase behavior, 3-D structural evolution, and assembly of binary mixtures with varying interactions.

Acknowledgment. This material is based on work supported by the U.S. Department of Energy, Division of Materials Science under award nos. DEFG02-01ER45941 and DEFG02-91ER45439. We gratefully acknowledge S. Granick and R. Tilton for the use of their experimental facilities, S. Jeon for experimental assistance, and E. Luijten, K. Schweizer, C. Martinez, and J. Gilchrist for useful discussions. A.T.C. has been partially supported by an NSF Graduate Research Fellowship.

Supporting Information Available: Modeling of interparticle interactions. This material is available free of charge via the Internet at <http://pubs.acs.org>.

LA0510073